

DNA-Induced Size-Selective Separation of Mixtures of Gold Nanoparticles

Jae-Seung Lee, Savka I. Stoeva, and Chad A. Mirkin*

Contribution from the Department of Chemistry and International Institute for Nanotechnology, Northwestern University, 2145 Sheridan Road, Evanston, Illinois 60208

Received March 9, 2006; E-mail: chadnano@northwestern.edu

Abstract: We present a novel method for size-selectively separating mixtures of nanoparticles in aqueous media utilizing the inherent chemical recognition properties of DNA and the cooperative binding properties of DNA-functionalized gold nanoparticles. We have determined that the melting temperatures (T_m s) of aggregates formed from nanoparticles interconnected by duplex DNA are dependent upon particle size. This effect is proposed to derive from larger contact areas between the larger particles and therefore increased cooperativity, leading to higher T_m s. The separation protocol involves taking two aliquots of a mixture of particles that vary in size and functionalizing them with complementary DNA. These aliquots are mixed at a temperature above the T_m for aggregates formed from the smaller particles but below the T_m for aggregates formed from the larger particles. Therefore, the aggregates that form consist almost exclusively of the larger particles and can be easily separated by sedimentation and centrifugation from the smaller dispersed particles. This unusual size-dependent behavior and separation protocol are demonstrated for three binary mixtures of particles and one ternary mixture.

Introduction

The concept of synthetically programmable assembly with oligonucleotides as particle directing groups has led to important advances in materials synthesis,¹ the development of powerful nucleic acid and protein diagnostic tools,² ways of assembling particles on single strand templates,³ and the discovery of fundamentally new properties for nanoparticles modified with DNA.⁴ In fact, many of the properties of oligonucleotide-modified nanoparticles not only derive from the DNA-coating on their surfaces but also the size of the particle used as a scaffold.^{4b,c,5} In general, particle size and size distribution play a significant role in controlling the properties of any colloid based upon a nanomaterial.⁶ As a result, many groups have developed a variety of approaches to achieve particle separation and to narrow the size distribution of particles in a colloidal

solution. Unlike molecular systems, it is often difficult to employ crystallization for colloidal structures, and the methods that have been used successfully are performed primarily in organic media. In such media, precipitation methods have been developed and used with great success for certain compositions.^{6a,b} Such methods, however, require an empirical tuning of the experimental conditions to effect optimum size-selective precipitation or crystallization. Other postsynthetic methods for refining particle size or separating a mixture of particles of different sizes in organic media include digestive ripening,⁷ use of supercritical fluids,⁸ gas pressurization,⁹ HPLC,¹⁰ and size-exclusion chromatography.¹¹

- (1) (a) Mirkin, C. A.; Letsinger, R. L.; Mucic, R. C.; Storhoff, J. J. *Nature* **1996**, *382*, 607–609. (b) Storhoff, J. J.; Mirkin, C. A. *Chem. Rev.* **1999**, *99*, 1849–1862. (c) Niemeyer, C. M. *Angew. Chem., Int. Ed.* **2001**, *40*, 4128–4158.
- (2) (a) Rosi, N. L.; Mirkin, C. A. *Chem. Rev.* **2005**, *105*, 1547–1562. (b) Taton, T. A.; Mirkin, C. A.; Letsinger, R. L. *Science* **2000**, *289*, 1757–1760. (c) Nam, J. -M.; Thaxton, C. S.; Mirkin, C. A. *Science* **2003**, *301*, 1884–1886. (d) Zhao, X.; Tapecc-Dytioco, R.; Tan, W. *J. Am. Chem. Soc.* **2003**, *125*, 11474–11475. (e) Liu, J.; Lu, Y. *J. Am. Chem. Soc.* **2003**, *125*, 6642–6643. (f) Weizmann, Y.; Patolsky, F.; Willner, I. *Analyst* **2001**, *126*, 1502–1504. (g) He, L.; Musick, M. D.; Nicewarner, S. R.; Salinas, F. G.; Benkovic, S. J.; Natan, M. J.; Keating, C. D. *J. Am. Chem. Soc.* **2000**, *122*, 9071–9077. (h) Wang, J.; Liu, G.; Merkoci, A. *J. Am. Chem. Soc.* **2003**, *125*, 3214–3215.
- (3) Alivisatos, A. P.; Johnsson, K. P.; Peng, X.; Wilson, T. E.; Loweth, C. J.; Bruchez, M. P.; Schultz, P. G. *Nature* **1996**, *382*, 609–610.
- (4) (a) Storhoff, J. J.; Lazarides, A. A.; Mucic, R. C.; Mirkin, C. A.; Letsinger, R. L.; Schatz, G. C. *J. Am. Chem. Soc.* **2000**, *122*, 4640–4650. (b) Jin, R.; Wu, G.; Li, Z.; Mirkin, C. A.; Schatz, G. C. *J. Am. Chem. Soc.* **2003**, *125*, 1643–1654. (c) Taton, T. A.; Lu, G.; Mirkin, C. A. *J. Am. Chem. Soc.* **2001**, *123*, 5164–5165.
- (5) Kiang, C.-H. *Physica A* **2003**, *321*, 164–169.

- (6) (a) Murray, C. B.; Kagan, C. R.; Bawendi, M. G. *Annu. Rev. Mater. Sci.* **2000**, *30*, 545–610. (b) Collier, C. P.; Vossmeier, T.; Heath, J. R. *Annu. Rev. Phys. Chem.* **1998**, *49*, 371–404. (c) El-Sayed, M. A. *Acc. Chem. Res.* **2004**, *37*, 326–333. (d) Alivisatos, A. P. *Science* **1996**, *271*, 933–937. (e) Park, J.; An, K.; Hwang, Y.; Park, J.-G.; Noh, H.-J.; Kim, J.-Y.; Park, J. -H.; Hwang, N.-M.; Hyeon, T. *Nat. Mater.* **2004**, *3*, 891–895. (f) Shevchenko, E. V.; Talapin, D. V.; Schnablegger, H.; Kornowski, A.; Festin, O.; Svedlindh, P.; Haase, M.; Weller, H. *J. Am. Chem. Soc.* **2003**, *125*, 9090–9101. (g) Sun, S.; Zeng, H. *J. Am. Chem. Soc.* **2002**, *124*, 8204–8205. (h) Xiong, Y.; Chen, J.; Wiley, B.; Xia, Y.; Aloni, S.; Yin, Y. *J. Am. Chem. Soc.* **2005**, *127*, 7332–7333. (i) Jana, N. R.; Peng, X. *J. Am. Chem. Soc.* **2003**, *125*, 14280–14281. (j) Wang, Z. L.; Harfenist, S. A.; Whetten, R. L.; Bentley, J.; Evans, N. D. *J. Phys. Chem. B* **1998**, *102*, 3068–3072. (k) Hussain, I.; Graham, S.; Wang, Z.; Tan, B.; Sherrington, D. C.; Rannard, S. P.; Cooper, A. L.; Brust, M. *J. Am. Chem. Soc.* **2005**, *127*, 16398–16399.
- (7) Stoeva, S.; Klabunde, K. J.; Sorensen, C. M.; Dragieva, I. *J. Am. Chem. Soc.* **2002**, *124*, 2305–2311.
- (8) (a) Shah, P. S.; Holmes, J. D.; Johnston, K. P.; Korgel, B. A. *J. Phys. Chem. B* **2002**, *106*, 2545–2551. (b) Clarke, N. Z.; Waters, C.; Johnson, K. A.; Satherley, J.; Schiffrin, D. *J. Langmuir* **2001**, *17*, 6048–6050.
- (9) McLeod, M. C.; Anand, M.; Kitchens, C. L.; Roberts, C. B. *Nano Lett.* **2005**, *5*, 461–465.
- (10) (a) Jimenez, V. L.; Leopold, M. C.; Mazzitelli, C.; Jorgenson, J. W.; Murray, R. W. *Anal. Chem.* **2003**, *75*, 199–206. (b) Wilcoxon, J. P.; Martin, J. E.; Provencio, P. *Langmuir* **2000**, *16*, 9912–9920.
- (11) Al-Somali, A. M.; Krueger, K. M.; Falkner, J. C.; Colvin, V. L. *Anal. Chem.* **2004**, *76*, 5903–5910.

In contrast, the improvement of the particle size distribution in aqueous media has been a more challenging task and is usually performed by filtration¹² or chromatographic methods such as size-exclusion chromatography¹³ and capillary electrophoresis.¹⁴ Such techniques, however, are somewhat limited in throughput and the types of compositions that can be used due to different degrees of interactions with column supports or filtration membranes (e.g., irreversible adsorption or membrane fouling) and the need for specialized equipment. For particles dispersed in aqueous media, it would be a major advance if one could utilize the inherent chemical recognition properties of biomolecules¹⁵ to size-selectively assemble particles. Herein, we describe a novel approach for the size-selective assembly and separation of nanoparticles in aqueous media. This approach takes advantage of the intrinsic particle size-dependent melting characteristics and the sharp melting profiles of oligonucleotide-functionalized gold nanoparticles (DNA–Au NPs),^{1,4b} and as a proof-of-concept, we demonstrate its utility for separating binary and ternary mixtures of gold particles.

Experimental Section

Functionalization of Au NPs with DNA. To investigate the particle size effect on the melting properties of NP aggregates, Au NPs with average diameters of 15, 30, 40, 50, 60, and 80 nm were studied. All Au colloids were purchased from Ted Pella. Two complementary HPLC-purified 5'-thiol-modified oligonucleotides (**a**, 5'-HS-(CH₂)₆-A₆-AGTGATAAG-3'; **b**, 5'-HS-(CH₂)₆-A₆-CTTATCACT-3') were obtained from Integrated DNA Technologies (IDT). The DNA functionalization of the Au NPs was performed following a previously published procedure with a few modifications.^{4b} DNA, freshly deprotected by dithiothreitol (DTT, Pierce) and purified by a NAP-5 column (GE Healthcare), was added to each Au colloid (final oligonucleotide concentration is ~6 μM), and the solution was brought to a concentration of 0.3 M NaCl in phosphate buffer (10 mM phosphate, 0.01% SDS, pH 7.4) through a stepwise process. The excess DNA was removed by repeated centrifugation and washing with a buffer solution (0.1 M NaCl, 10 mM phosphate, 0.005% Tween 20, pH 7.4).

Homoparticle Aggregate Formation. In each case, two samples of particles of the same size were functionalized with DNA sequences **a** and **b**, respectively, and combined (final concentration of each particle with a given DNA sequence was 100 pM in all cases). The mixture was heated at 50 °C for 10 min and allowed to hybridize under the hybridization conditions (room temperature, 0.1 M NaCl, 10 mM phosphate, 0.005% Tween 20, pH 7.4). The particle concentrations were measured by UV–vis spectroscopy (Cary 5000, Varian) using the molar extinction coefficients at the wavelength of the maximum absorption of each gold colloid [$\epsilon_{(15)528\text{nm}} = 3.6 \times 10^8 \text{ cm}^{-1} \text{ M}^{-1}$, $\epsilon_{(30)530\text{nm}} = 3.0 \times 10^9 \text{ cm}^{-1} \text{ M}^{-1}$, $\epsilon_{(40)533\text{nm}} = 6.7 \times 10^9 \text{ cm}^{-1} \text{ M}^{-1}$, $\epsilon_{(50)535\text{nm}} = 1.5 \times 10^{10} \text{ cm}^{-1} \text{ M}^{-1}$, $\epsilon_{(60)540\text{nm}} = 2.9 \times 10^{10} \text{ cm}^{-1} \text{ M}^{-1}$, and $\epsilon_{(80)550\text{nm}} = 6.9 \times 10^{10} \text{ cm}^{-1} \text{ M}^{-1}$].¹⁶

Melting Analyses. Melting analyses of the hybridized Au colloids were performed by monitoring the change in extinction at 260 nm every

0.2 °C at a rate of 1 °C min⁻¹ (Cary 5000 equipped with a Peltier temperature controller, Varian). For homogeneity, the solution was continuously stirred with a magnetic stir bar. The melting temperatures (T_{ms}) were derived from the maximum of the first derivatives of the melting transitions.

Size-Selective Separation of Binary Mixtures (30/60, 15/60, and 40/80 nm). In a typical experiment, unmodified 30 and 60 nm particles were mixed in a 1:1 ratio. The NP mixture was divided into two aliquots and modified with oligonucleotides (**a** and **b**, respectively) following the same procedure established for a single component system (vide supra). The two aliquots of 30/60 nm particles functionalized with DNA sequences **a** and **b**, respectively, were combined (each particle with a given DNA sequence was at a final concentration of 100 pM, $\epsilon_{(30/60)540\text{nm}} = 1.6 \times 10^{10} \text{ cm}^{-1} \text{ M}^{-1}$),¹⁶ heated to 50 °C for 10 min, and then held at 44 °C for 4 days to allow selective DNA–Au NP hybridization. The homoparticle aggregates composed of the 60 nm particles through the particle size-selective hybridization process were isolated by centrifugation (1000 rpm for 2 min). The supernatant containing the 30 nm particles was decanted from the precipitate. The precipitate was washed with a buffer solution twice (0.1 M NaCl, 10 mM phosphate, 0.005% Tween 20, pH 7.4). The supernatant was additionally centrifuged at 3000 rpm for 2 min, and any precipitate was discarded. Two other particle mixture combinations (15/60 nm and 40/80 nm) were separated under the same conditions [$\epsilon_{(15/60)537\text{nm}} = 1.3 \times 10^{10} \text{ cm}^{-1} \text{ M}^{-1}$ and $\epsilon_{(40/80)545\text{nm}} = 3.6 \times 10^{10} \text{ cm}^{-1} \text{ M}^{-1}$].¹⁶

Size-Selective Separation of a Ternary Mixture (30/50/80 nm).

The size-selective separation of a ternary mixture was performed in a similar manner as the binary mixtures. Unmodified 30, 50, and 80 nm gold particles were mixed in a 1:1:1 ratio. The NP mixture was divided into two aliquots and modified with oligonucleotides (**a** and **b**, respectively) following the same procedure established for a single component system (vide supra). The two aliquots of 30/50/80 nm particles functionalized with DNA sequences **a** and **b**, respectively, were combined (each particle with a given DNA sequence was at a final concentration of 35 pM, $\epsilon_{(30/50/80)542\text{nm}} = 3.1 \times 10^{10} \text{ cm}^{-1} \text{ M}^{-1}$),¹⁶ heated to 50 °C for 10 min, and then held at 45 °C for 3 days to allow the first selective hybridization (80 nm NPs). The 80 nm homoparticle aggregates were isolated by centrifugation (1000 rpm for 2 min) and washed with a buffer solution twice (0.1 M NaCl, 10 mM phosphate, 0.005% Tween 20, pH 7.4). The supernatant containing the 50 and 30 nm particles was centrifuged at 3000 rpm for 2 min to discard any precipitate and held at 43 °C for the second size-selective hybridization (50 nm NPs). After 3 days, the 50 nm homoparticle aggregates were isolated by centrifugation (1000 rpm for 2 min) and washed with a buffer solution twice (0.1 M NaCl, 10 mM phosphate, 0.005% Tween 20, pH 7.4). The supernatant containing the 30 nm particles was additionally centrifuged at 3000 rpm for 2 min, and any precipitate was discarded. Note that the hybridization time for each separation step for this ternary mixture (3 days) was shorter than that used for the binary mixtures (4 days).

Fluorophore-Labeled DNA Coverage Study. The DNA coverage on the Au NP surface was determined by functionalization of the Au NPs with fluorophore-labeled DNA.¹⁷ Six types of Au colloids (15, 30, 40, 50, 60, and 80 nm diameter, Ted Pella) were functionalized with 3'-fluorophore-labeled 5'-thiol-modified sequence **b** (5'-HS-(CH₂)₆-A₆-CTTATCACT-(6-FAM)-3', Integrated DNA Technologies). Freshly deprotected DNA was added to each Au colloid (final oligonucleotide concentration is ~6 μM). The salt concentration was brought to 0.3 M NaCl in phosphate buffer (10 mM phosphate, 0.01% SDS, pH 7.4) following the stepwise salting procedure (vide supra). The colloids were washed four times with a buffer solution (0.3 M NaCl, 10 mM phosphate, 0.005% Tween 20, pH 7.4) by centrifugation and finally

- (12) Sweeney, S. F.; Woehrl, G. H.; Hutchison, J. E. *J. Am. Chem. Soc.* **2006**, *128*, 3190–3197.
 (13) (a) Wei, G.-T.; Liu, F.-K. *J. Chromatogr. A* **1999**, *836*, 253–260. (b) Novak, J. P.; Nickerson, C.; Franzen, S.; Feldheim, D. L. *Anal. Chem.* **2001**, *73*, 5758–5761.
 (14) Templeton, A. C.; Cliffl, D. E.; Murray, R. W. *J. Am. Chem. Soc.* **1999**, *121*, 7081–7089.
 (15) (a) Dillenback, L. M.; Goodrich, G. P.; Keating, C. D. *Nano Lett.* **2006**, *6*, 16–23. (b) Mann, S.; Shenton, W.; Li, M.; Connolly, S.; Fitzmaurice, D. *Adv. Mater.* **2000**, *12*, 147–150. (c) Niemeyer, C. M.; Simon, U. *Eur. J. Inorg. Chem.* **2005**, 3641–3655. (d) Gole, A.; Murphy, C. J. *Langmuir* **2005**, *21*, 10756–10762. (e) Claridge, S. A.; Goh, S. L.; Frechet, J. M. J.; Williams, S. C.; Micheel, C. M.; Alivisatos, A. P. *Chem. Mater.* **2005**, *17*, 1628–1635.
 (16) The molar extinction coefficients are calculated from the measured UV–vis absorbance of a colloid with a known particle concentration.

- (17) Demers, L. M.; Mirkin, C. A.; Mucic, R. C.; Reynolds, R. A.; Letsinger, R. L.; Enghanian, R.; Viswanadham, G. *Anal. Chem.* **2000**, *72*, 5535–5541.

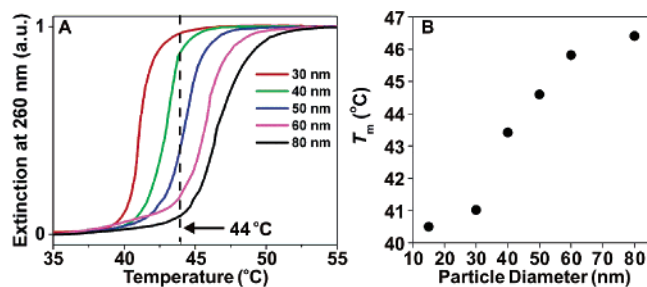


Figure 1. (A) Normalized melting curves of each homoparticle aggregate. The melting curve for the aggregates formed from the 15 nm NPs is not shown because of the low extinction coefficient for this size particle. (B) A graph of T_m s for the aggregates as a function of NP size. Note that a 10 nm difference in diameter leads to ~ 1.5 °C change in T_m . This effect is minimized at the small (15 nm) and large (80 nm) ends of the particle size range. This observation could be correlated to the slightly higher DNA surface coverage for the 15 nm NPs and slightly lower DNA surface coverage for the 80 nm NPs compared to the coverages for the intermediate sized particles (see Figure 4).

redispersed in the same buffer. The particle concentration in each colloid was measured by UV–vis spectroscopy (Cary 5000, Varian).

The fluorophore-labeled DNA strands were released from the Au NPs by a ligand exchange process induced by DTT (final DTT concentration was 0.5 M).¹⁸ After DTT addition, the solutions were incubated at 50 °C for 5 min and held at room temperature for 1 h. The solutions were centrifuged at 10 000 rpm for 15 min to isolate the Au NPs, and the supernatants containing the released fluorophore-labeled DNA strands were collected for the fluorescence analyses.

A series of dilutions (0.50, 1.0, 2.0, 3.0, 6.0, 8.0, 10, 20, 25, 50, and 100 nM) of the fluorophore-labeled DNA were prepared in 0.5 M DTT solution in phosphate buffer (0.3 M NaCl, 10 mM phosphate, 0.005% Tween 20, pH 7.4) to obtain a standard calibration curve (see Supporting Information, Figure 1S). The fluorescence of the DNA samples was measured in a 96-well plate format using a Gemini EM fluorescence/chemiluminescence plate reader (Molecular Devices). The number of DNA strands per particle was calculated from the measured fluorescence intensity and the standard calibration curve. The density of DNA strands on the Au NP surface for each particle size was obtained from the number of DNA strands per particle (see Supporting Information, Table 1S) and the surface area of the particle. Five separate experiments were performed for each particle size.

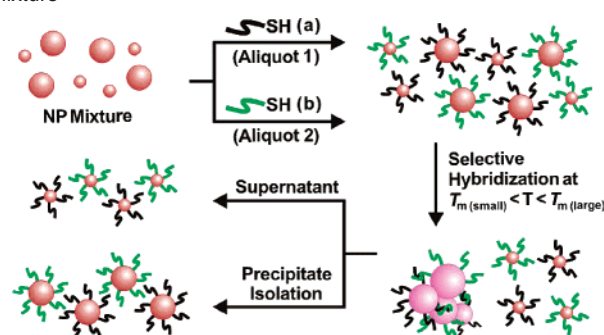
Transmission Electron Microscopy. Samples for TEM were prepared by placing a 3 μ L drop of the solution onto a carbon-coated Formvar copper grid (300 mesh, Electron Microscopy Sciences). The grids were allowed to dry in a dust free area. TEM images were obtained on a Hitachi 8100 operating at 200 kV.

Results and Discussion

Particle Size Effect on T_m s of Homoparticle Aggregates.

It has been suggested that DNA–Au NPs, when hybridized to complementary particles of the same diameter, exhibit T_m s that are dependent upon particle size.⁵ We hypothesized that if the particle aggregates formed from DNA-directed assembly exhibited significant changes in T_m , one could use temperature and programmable assembly methods to separate a mixture of particles that differed in size. To evaluate this hypothesis, we have studied the magnitude of the T_m difference for a series of homoparticle aggregates each formed from particles of a different size (15, 30, 40, 50, 60, and 80 nm particles) but assembled with the same duplex DNA interconnects under identical conditions. As shown in Figure 1A, the observed

Scheme 1. DNA-Induced Size-Selective Separation of a NP Mixture



melting behavior of each homoparticle aggregate is highly dependent on the size of the NPs. Interestingly, as the particle size increases, there is a significant and measurable increase in T_m for all particle sizes studied. For example, aggregates composed of 15 nm particles melt at 40.5 °C, while 80 nm NP aggregates melt at 46.4 °C (Figure 1B).

Size-Selective Separation of Binary and Ternary NP Mixtures. Because of these T_m differences and the sharp, highly cooperative melting transitions, which are characteristic of aggregates formed from these NP–DNA conjugates, we hypothesized that mixtures of particles of different sizes could be separated by size-selective hybridization at a specific temperature that is between the T_m s of each homoparticle aggregate (Scheme 1). Such conditions are expected to result in the hybridization of the large particles, leaving the small particles in the supernatant. To test this hypothesis, we prepared three different particle mixtures consisting of particles of two different sizes and explored their hybridization properties. In the case of the 30/60 nm particle mixture, 44 °C was chosen as a size-selective hybridization temperature, because it is on the higher plateau of the melting curve of the 30 nm homoparticle aggregates and on the lower plateau of the melting curve of the 60 nm homoparticle aggregates (Figure 1A). At the end of the experiment, aggregates of 60 nm particles formed exclusively, leaving 30 nm particles dispersed in the supernatant. This size selective hybridization was then demonstrated for two other particle size combinations (15/60 and 40/80 nm). Mixtures of 15/60 and 40/80 nm NPs were similarly size-selectively hybridized and separated, because 44 °C is also between the T_m s of the small (15 and 40 nm) and the large (60 and 80 nm) homoparticle aggregates in both cases. For all combinations, the particles in the collected aggregates dissociated upon water addition or heating with a concomitant color change of the solution to red. Importantly, for each combination we do not expect the formation of heteroparticle aggregates composed of small and large particles at 44 °C, because the T_m s of such aggregates are all below this temperature (see Supporting Information, Figure 2S). Moreover, simple centrifugation of unmodified Au NPs under similar experimental conditions did not yield precipitates. The 4 day assembly period was determined by monitoring the hybridization rate of 60 nm DNA–Au NPs (each at 100 pM concentration) at 44 °C by measuring the change in extinction of the colloid at 260 nm, which is diagnostic for the particle assembly process (see Supporting Information, Figure 3S).^{4b}

Representative transmission electron microscopy (TEM) images of each sample before and after the size-selective

(18) Thaxton, C. S.; Hill, H. D.; Georganopoulou, D. G.; Stoeva, S. I.; Mirkin, C. A. *Anal. Chem.* **2005**, *77*, 8174–8178.

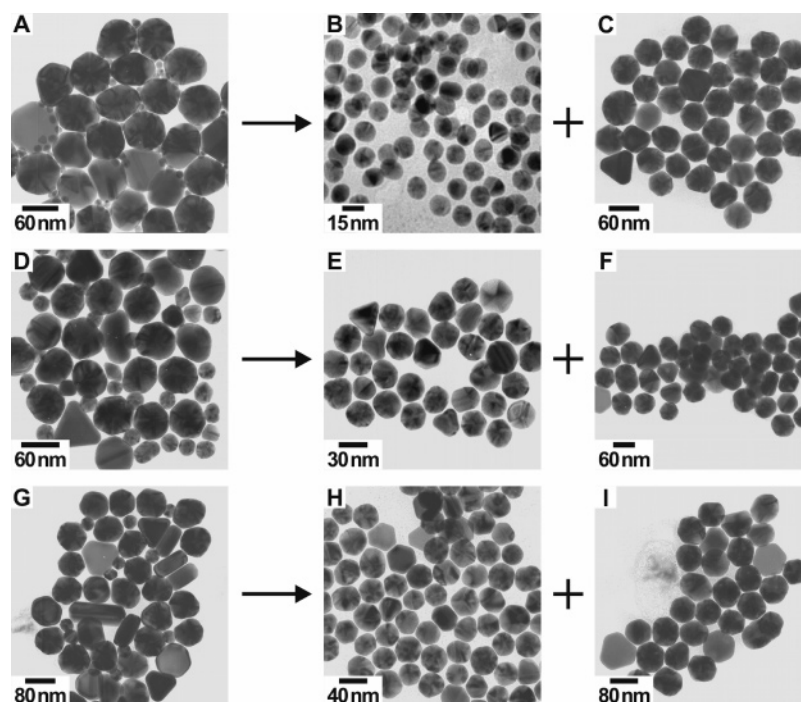


Figure 2. Representative TEM images of DNA–Au NPs before and after the size-selective separation of binary particle mixtures: (A) 15/60 nm, (B) 15 nm, (C) 60 nm, (D) 30/60 nm, (E) 30 nm, (F) 60 nm, (G) 40/80 nm, (H) 40 nm, (I) 80 nm. Note that the length scale is different in each of the images. Additional representative TEM images are shown in Supporting Information (Figure 4S).

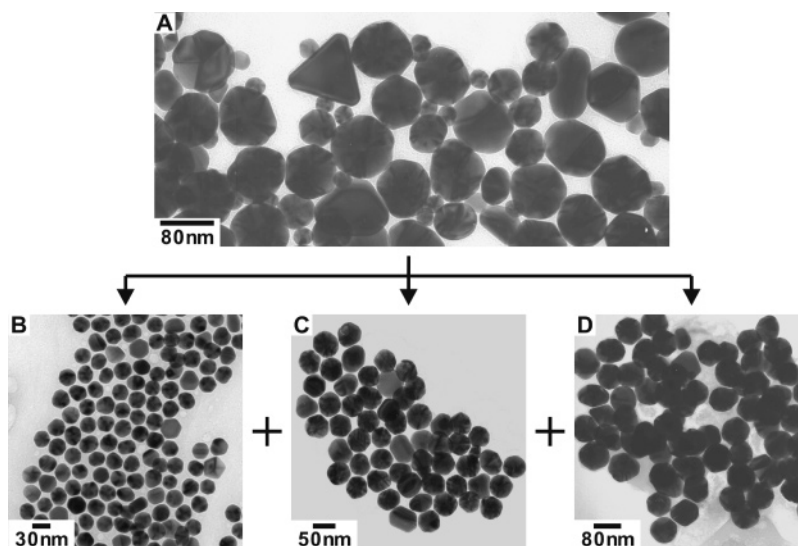


Figure 3. Representative TEM images of DNA–Au NPs before and after the size-selective separation from a ternary mixture: (A) the starting mixture of 30, 50, and 80 nm particles, (B) the separated 30 nm particles, (C) the separated 50 nm particles, and (D) the separated 80 nm particles.

hybridization and separation protocol are shown in Figure 2. In each case the particles are separated with nearly 100% efficiency into the corresponding small (15, 30, and 40 nm) and large (60 and 80 nm) particles. As predicted, the precipitates are composed of the large particles and the supernatants contain only the small particles. A few small particles (<1%) were found in the precipitates and a few large particles (<5%) in the supernatants without the additional washing step, indicating that only large particles took part in the hybridization and the small particles merely remained in the supernatant without being hybridized.

We further evaluated the potential for particle size-selective hybridization to be used in the separation of a mixture composed of three different particle sizes (30, 50, and 80 nm, Figure 3A).

The separation was performed in a stepwise manner starting with the hybridization and isolation of the largest NPs (80 nm) by holding the temperature of the mixture at 45 °C. This temperature was chosen because it is below the T_m of the homoparticle aggregates formed from the 80 nm particles and above those for the 30 and 50 nm homoparticle aggregates. The aggregate that forms under these conditions is composed almost exclusively of the 80 nm particles (Figure 3B), and the supernatant contains the 30 and 50 nm particles. The remaining mixture of 30 and 50 nm particles could be separated using the binary mixture separation protocol described above. Parts B, C, and D of Figure 3 illustrate representative TEM images of the isolated 30, 50, and 80 nm particles, respectively, after the size-selection process. A thorough investigation of 15 TEM

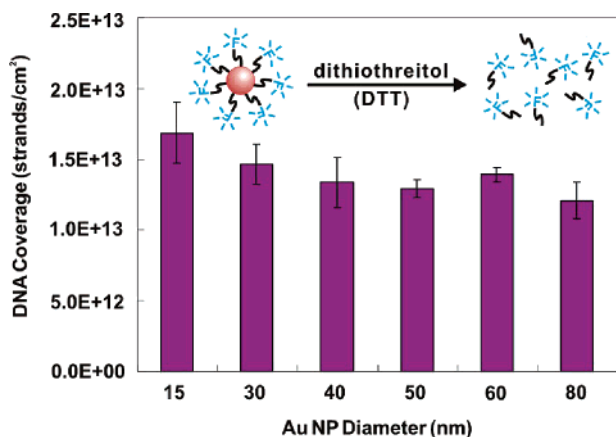


Figure 4. The DNA surface coverage for each particle size, as determined by fluorophore labeling experiments.

images for each NP size shows a separation efficiency of more than 90% in each case.

The Chemical and Physical Origin of the Size-Selective Hybridization Process. This size-selective phenomenon is directly related to the number of duplex DNA connections formed between each particle, which is determined by the DNA density on the particle surface and the particle–particle contact area. The NPs are designed to directly hybridize with one another through a complementary two-strand system. The number of duplex particle interconnects will depend on particle–particle contacts and oligonucleotide surface coverage. The DNA surface coverage for each particle size was determined using fluorophore-labeled DNA and found to be similar regardless of the NP size ($\sim 1.4 \times 10^{13}$ DNA strands/cm², Figure 4). Therefore, we believe the particle–particle contact area to be the dominant contributor to the effects we are reporting and utilizing in our size-dependent separation scheme. The larger particles, which have larger contact area with the surrounding particles, form a larger number of DNA duplex interconnects between the particles that comprise the aggregates. Therefore, the aggregates composed of larger particles melt at higher temperature, because the number of linkages between the particles proportionally influences the melting enthalpy due to

cooperative melting interactions.^{4b} Other independent theoretical studies also are consistent with the conclusion that multiple closely spaced linkages are responsible for the increased T_m associated with DNA-assembled particle aggregates.¹⁹

Conclusion

We have developed a novel method for the size-selective separation of Au NPs in aqueous media. This method can be viewed as a type of synthetically programmable “recrystallization” process that is guided by the chemical recognition properties of DNA. Its limitations are that it requires a DNA-modification step, appropriate time for the size-selective hybridization, and improvement of separation resolution (at present, 20 nm compared to less than 10 nm demonstrated by chromatographic and filtration methods). However, its strengths are that it can be tailored for mixtures of particles that vary in size simply through the choice of the DNA interconnect and desired recrystallization conditions (e.g., temperature, salt concentration). Importantly, in principle, this is an approach that can be generalized for the separation of other types of NPs that can be readily functionalized with DNA and to more complex systems composed of particles that differ in size and shape.²⁰

Acknowledgment. C.A.M. acknowledges AFOSR, DARPA, and NSF for generous support of this work. He is also grateful for a NIH Director’s Pioneer Award. Dr. Min Su Han is acknowledged for helpful discussions.

Supporting Information Available: Additional representative TEM images for the binary mixture separations, melting curves of heteroparticle aggregates, the number of DNA strands on Au NPs of different sizes, and the hybridization rate of 60 nm DNA-Au NPs. This material is available free of charge via the Internet at <http://pubs.acs.org>.

JA061651J

- (19) (a) Park, S. Y.; Stroud, D. *Phys. Rev. B* **2003**, *67*, 212202. (b) Park, S. Y.; Stroud, D. *Phys. Rev. B* **2003**, *68*, 224201.
- (20) (a) Millstone, J. E.; Park, S.; Shuford, K. L.; Qin, L.; Schatz, G. C.; Mirkin, C. A. *J. Am. Chem. Soc.* **2005**, *127*, 5312–5313. (b) Mbindyo, J. K. N.; Reiss, B. D.; Martin, B. R.; Keating, C. D.; Natan, M. J.; Mallouk, T. E. *Adv. Mater.* **2001**, *13*, 249–254. (c) Dujardin, E.; Hsin, L.-B.; Wang, C. R. C.; Mann, S. *Chem. Commun.* **2001**, 1264–1265.